ated with recurrent lupus enteritis and peritonitis. Clin Rheumatol 23：351-354，2004
13) Mariq HR et al：Prevalence of scleroderma spectrum disorders in the general population of South Carolina. Arthritis Rheum 32：998-1006，1989
14) LeRoy EC et al：Increased collagen synthesis by scleroderma skin fibroblasts in vitro；a possible defect in the regulation or activation of the scleroderma fibroblast. J Clin Invest 54：880-889，1974
15) Nelson JL et al：Microchimerism and HLA-compatible relationships of pregnancy in scleroderma. Lancet 351：559-562，1998
16) LeRoy EC et al：Scleroderma（systemic sclerosis）；classification，subsets and pathogenesis. J Rheumatol 15：202-205，1988
17) Kuwana M et al：Clinical and prognostic associations based on serum antinuclear antibodies in Japanese patients with systemic sclerosis. Arthritis Rheum 37：75-83，1994
18) Moore HC et al：The kidney of scleroderma. Lancet 1：68-70，1952
19) Medsger TA et al：Survival with scleroderma. II. A life-table analysis of clinical and demographic factors in 358 male U.S. veteran patients. J Chronic Dis 26：647-660，1973
20) Kono H et al：Pneumomediastinum in dermatomyositis association with cutaneous vasculopathy. Ann Rheum Dis 59：372-376，2002
21) 東條　毅：混合性結合組織病の治療指針. p4-9，1996
22) 近藤有好：膠原病の肺病. 内科 55：665-670，1985
23) Jennetts JC et al：Nomenclatire of systemic vasculiticles，Proposal of International Consensus Conference. Arthritis Rheum 37：187-192，1994
24) Sugai S：Sjögren syndrome. Nippon Naika Gakkai Zasshi 88：1896-1903，1999
25) Voulgarelis M et al：Malignant lymphoma in primary Sjögren's syndrome；a multicenter，retrospective，clinical study by the European Concerted Action on Sjögren's Syndrome. Arthritis Rheum 42：1765-1772，1999

Summary

The summary of image findings of autoimmune diseases

Because autoimmune diseases form a spectrum of affecting systemic disorders with involvement of many organs，there is a wide range of image findings. Imaging diagnosis plays an important role in recognizing the condition and identifying the associated autoimmune diseases. Here we comment on the classification and recent topics concerning collagen diseases. Furthermore，we review the image findings for each organ.

Kayo Sagawa et al
Department of Allergy and Rheumatology
University of Tokyo

自己免疫疾患における中枢神経病変
—MRIを中心に—

徳丸阿耶*

はじめに

免疫系は自己の成分に対して，決して反応してはならない機構である。その基本的役割は，外界から侵入するものを認識し攻撃することで，自らの個体を守ることにある。この免疫機構が破綻し，自己の細胞や組織のもつ抗原に対して自己抗体を作り出すことで起こる病気が，自己免疫疾患である。慢性関節リウマチ，全身性エリテマトーデスなど自己免疫疾患の多くは，全身を侵しうるもので，臨床症状も多彩であることが知られている。また，多くの疾患群で中枢神経系にも病変が認められ，予後やQOLに多大な影響を与える因子となる。画像診断は，病態の把握に非常に大切で，また有用なツールであるが，同時にその所見は非特異的でしかなく，診断に苦慮する場合も多い。すべての疾患を網羅することはかなわないが，できるだけ多くの画像を提示し役立てていただくことを本稿の目的としたい。

1. 膠原病

病理組織学的に血管，結合織にフィブリノイド変性が認められる一連の疾患群を膠原病とよぶ。全身の結合組織が侵され多数の臓器が障害される病気で，SLE，リウマチ熱，慢性関節リウマチ，強皮症，多発性筋炎，皮膚筋炎，結節性多発動脈炎，シェーグレン症候群などが含まれ自己免疫疾患の多くを占めている。原因不明の発熱や，関節痛など炎症に基づく臨床症状など共通項も多いが，一つ一つは独立した疾患として，特徴的症状や治療法を有する。近年特異抗原や遺伝子検索などの追及がさらに進み，それぞれの病因に基づいての疾患の見直しも始まっている。本稿では，全身性エリテマトーデス（SLE），シェーグレン症候群（Sjögren syndrome：SjS），動脈炎のいくつかを取り上げる。

膠原病1：全身性エリテマトーデス（systemic lupus erythematosus：SLE）

SLEは，膠原病の代表的疾患である。原因は不明だが，多種類の自己抗体が検出され，自己免疫疾患と考えられている。男女比は1：9と圧倒的に女性に多く，また若年者に多い。再発緩解を繰り返す全身臓器を侵しうる疾患で，画像診断に際しても臨床症状の確認は大切である。顔面の蝶形紅斑などの皮膚症状，関節炎，心臓，腎臓などを侵す。SLE患者における血栓性病態に抗カルジオリピン抗体やlupus anticoagulantなどの抗リン脂質抗体が密接に関連していることが明らかになり，抗リン脂質抗体症候群という新たな疾患概念が確立された。臨床的には，動静脈血栓症や習慣性流産などが認められ，検査所見として抗リン脂質抗体が検出される。膠原病，特にSLEに合併する例がもっとも多いが，

* A.M. Tokumaru　東京都老人医療センター放射線科
〔索引用語：自己免疫疾患〕

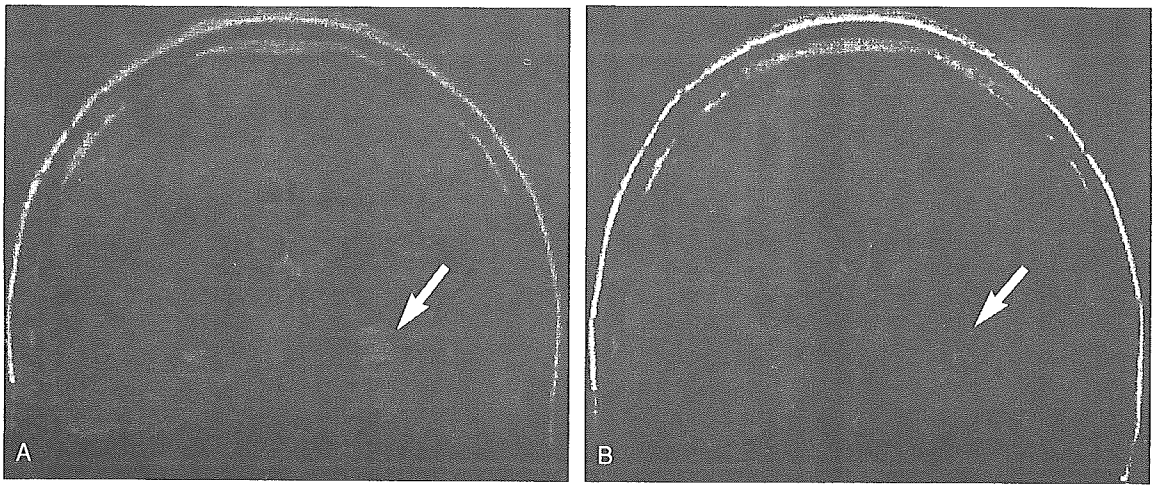

図1　30歳女性　SLE，意識混濁
A　FLAIR冠状断　左視床外側に不正形の高信号強度が捉えられる（→）。B　ステロイドパルス療法後　信号強度異常は消失している（→）。

若年では既知の膠原病や明らかな基礎疾患を有さない例の報告も認められる。血小板減少もしばしば認められ，抗リン脂質抗体症候群診断の切っ掛けになる事も多い。

SLEの中枢神経障害は，CNS-lupusとしてしられ，報告によって幅はあるが，20～70%と高率に認められる。中枢神経障害の有無とコントロールは，予後，QOL向上に重要な因子であり，画像所見の正確な把握は必要不可欠な事項である。

画像所見

この所見があればSLEという特異的な画像所見を取り上げることは困難で，画像所見は多彩であることを十分に承知しておく必要がある。血管周囲への炎症細胞浸潤，血管壁障害などに基づく病巣は，小梗塞，小出血，血管周囲の炎症，これに基づく血栓形成などをきたす[1]。それぞれの病態に応じた画像所見を呈する訳だが，白質にみられる血管周囲炎を示唆する病巣は，T2強調像，FLAIR画像で高信号を示す斑状病巣としての報告が多い。病巣は，ときに造影増強効果を示すが，その際血管周囲や髄膜の造影増強効果を伴うこともあり，病態を考える上でのヒントとなる。経過観察によって，画像所見の軽快が認められることがあるが，血管性浮腫がその機序として考慮されている。また，SLEは抗リン脂質抗体症候群の基礎疾患として捉えられる場合も多い。抗リン脂質抗体症候群を合併する例では，血栓症を頻繁にきたすことが知られている[2) 3)]。通常SLEでは中小から毛細血管レベルでの障害とされるが，抗リン脂質抗体症候群合併例では，図4で示したように大血管での閉塞をきたす場合もあり留意を要する。MRAでの血管評価を必要とする場合もあると考えられる。

図1は，30歳女性。家族を認識できないなど意識混濁が認められる。FLAIR画像で左視床外側に不正形の高信号強度が認められる。ステロイドパルス療法後症状は消失し，異常信号も消失している。

図2は，43歳女性。歩行障害，意識変容を示す。FLAIR画像で両側放線冠にびまん性に淡い高信号領域を認める。前者は今回のエピソードをきっかけにSLEの診断がなされた例である。他の臨床症状や検査所見からSLEと診断がついている場合は，これらの白質病変とSLEとの関連を考慮することは可能だが，画像所見は非特異的で他の白質脳症，血管炎，あるいは感染性脳炎なども含めて鑑別を迫られる場合もありうる。

図3は，37歳女性。抗リン脂質抗体症候群を伴うSLE例で，T2*画像で，皮質下，基底核部など

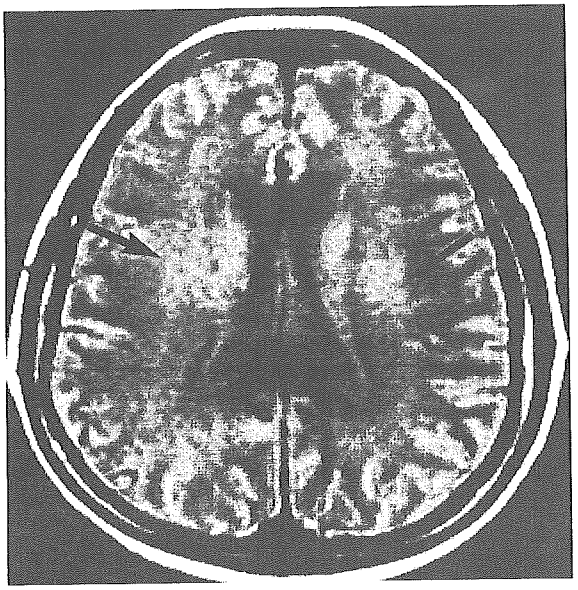

図2　43歳女性　歩行障害，意識変容　FLAIR横断画像
両側皮質下から深部白質に淡い高信号強度の広がりが認められる（→）。

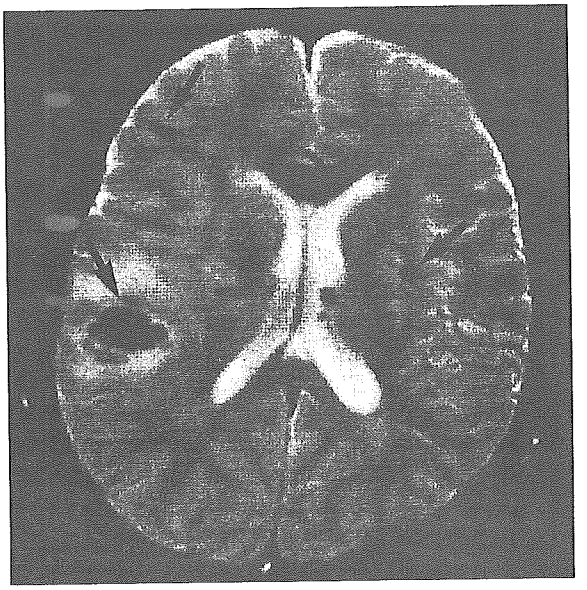

図3　37歳女性　抗リン脂質抗体症候群を伴うSLE
TIA様の発作を繰り返している。T2*強調像では皮質下，基底核部などに多数の低信号強度が認められ，多発出血性病巣と考えられる（→）。

に多発の出血性病巣が指摘される。

比較的若年女性の梗塞，出血に際して，危険因子としての膠原病のチェック，抗リン脂質抗体のチェックは必須事項である。

膠原病 2：シェーグレン症候群（Sjögren syndrome：SjS）

シェーグレン症候群は，自己免疫疾患（膠原病）の一つで，主に唾液腺や涙腺などの外分泌腺の慢性炎症をきたす。欧米を含めれば，膠原病で最も頻度が高い。患者さんは目の乾燥，口渇，虫歯ができやすいなどの症状を訴え，中年以降の女性に多い。慢性関節リウマチなど他の膠原病疾患との合併例は二次性SjS，合併がないものを一次性SjS（primary SjS）とよぶ。14～25%の中枢神経障害合併が報告され，QOL，予後に重要な因子となる。中枢神経症状が初発の症例も経験され，中高年女性の白質病変，脊髄炎などをみた場合に原因疾患としての一考を要する。ステロイド治療が奏功する場合もあり，基礎疾患の示唆は大切である。発症機序として，中枢神経系への単核球浸潤，血管炎（血管周囲炎），脳血管スパスムなどが報告されている。

画像所見

皮質下白質や，深部白質にT2強調像，FLAIR画像で高信号を示す小病巣が孤発あるいは多発性に認められる[4-7]。時に造影増強効果を示す。時間的多発が認められることもあり，多発性硬化症との異同がしばしば問題になる[5]。脊髄病変，視神経炎の報告もあり[8]，中高年以上の女性で，原因不明の白質病変，脊髄炎疑い病変などが認められた場合，SjSの可能性も一考することには意義がある。

図5A，Bは，63歳女性。左上下肢の痺れを訴えた時点のMRI，T2強調横断画像である。右大脳脚を含む中脳右腹側にわずかに腫脹する高信号病変，右内包後脚，外包に及ぶ高信号を示す病変が認められる。ステロイド治療が選択され，症状は一過性に軽快をみたが，6カ月後，再び右上下肢の脱力などの訴えが認められた。この際のMRI検査で，右大脳脚病巣は縮小しているのにかかわらず，対側錐体路に沿う帯状の高信号が新たに出現している（図5C）。白質線維束に沿

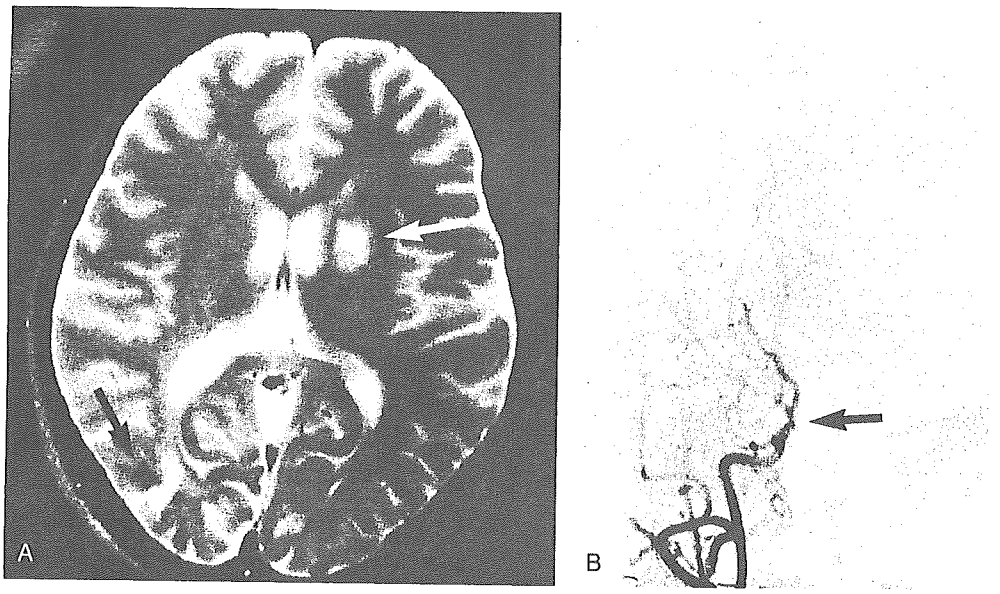

図4　34歳女性　抗リン脂質抗体症候群を伴うSLE
A　T2強調横断画像　右即答高等に低信号と高信号の混在する病巣（黒→）が認められ，左被殻には不正形の高信号強度（白→）が認められる。複数の出血，梗塞の存在が疑われる。B　右内頸動脈造影正面像　右中大脳動脈，前大脳動脈分岐での壁不正，高度狭窄が認められる（→）。

う病巣の局在は，たんに小梗塞と断定するには非典型的であり，病態を考えるヒントとなる所見である。また，本例は経過中に左視力障害を生じ，その際のMRIでは左視神経にT2強調像で高信号強度が捉えられる（図5D）。このように，SjSに視神経炎を合併する症例も報告が散見される[8]。

図6は，54歳女性。C3～6椎体レベルの髄内には，T2強調像で淡い高信号を示す病巣が認められる（図6A）。本例も，右大脳脚にかかる部位にT2強調像での高信号強度が捉えられ，一部に造影増強効果が捉えられた（図6B，C）。脊髄炎を合併し，また病巣に造影増強効果を示す場合もある。病巣の局在，時間的空間的多発，視神経炎合併など多発性硬化症（multiple sclerosis：MS）との鑑別を要する。

2. ANCA related angitis（ANCA関連血管炎）

膠原病で中枢神経症状を呈する血管炎として結節性多発動脈炎がよく知られているが，近年，血管炎症候群の再分類が提唱されていることを踏まえ，本稿ではANCA関連血管炎として取り上げ解説を試みたい。血管炎症候群の分類はこれまで，侵される血管径と臨床像の特徴によってなされてきた。大動脈，幹動脈を侵すものが高安動脈炎，側頭動脈炎であり，中小筋型動脈が侵されるものが，結節性多発動脈炎，Wegener肉芽腫（WG），Churg-Strauss症候（CSS）などである。結節性多発動脈炎のうち，中等度の血管を侵すものが古典型，小動脈から毛細血管，細静脈を侵すものを顕微鏡的多発血管炎として区別されてきた。近年，抗好中球細胞質抗体（antineutrophil cytoplasmic antibodies：ANCA）が同定され，従来の臨床像のみでなく，ANCAとの関連による分類を組み合わせることが提唱され始めている。

なぜANCAが産生され，発症するのか，その詳細は不明だが，ANCAの対応抗原は好中球ライソゾーム顆粒であり，いずれの酵素も組織障害性が強く，血管内皮融解ひいては，壊死性血管炎発症との関連が考慮されている。ANCA関

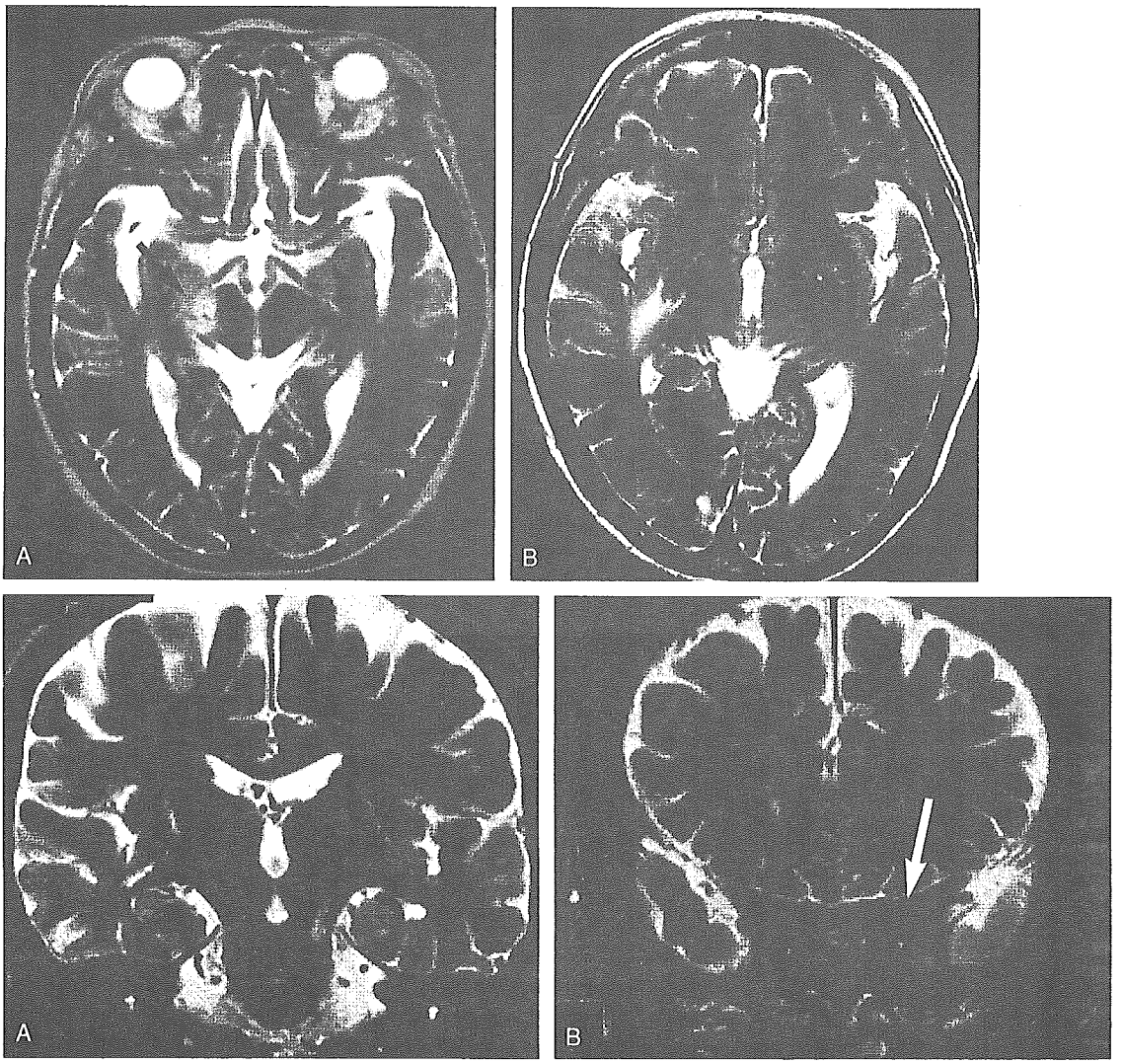

図5　63歳女性　SjS　消長を繰り返す左上下肢しびれ，左視力障害
A　T2強調横断画像（TR/TE＝4000/120）右大脳脚部に腫脹を伴う高信号強度がとらえられる（→）。B　T2強調横断画像（TR/TE＝4000/120）右内包後脚，外包にそって広がる高信号強度が認められる（→）。C　左上下肢の症状軽快後6カ月　T2強調冠状断画像（TR/TE＝4000/120）新たに右上下肢痺れが出現。右大脳脚の病巣はほぼ消失しているが，左錐体路にそって帯状の高信号強度が出現している（→）。D　T2強調冠状断画像（TR/TE＝4000/120）左視力は光覚弁。→で示す左視神経は信号上昇を示す。

連血管炎には，WG，CSS，MPAが含まれる。またANCAには，細胞質にびまん性に顆粒状の蛍光を認めるc-ANCA（cytoplasmic ANCA）と，核周辺に蛍光を認めるp-ANCA（perinuclear ANCA）の2つの染色型があることが知られ，それぞれの対応抗原が異なる。c-ANCAは，WGに疾患特異性が高い。p-ANCAの疾患特異性はやや低いものの，MPA，CSS，特発性壊死性半月体形成性腎炎などに陽性を示す。まれに，p-ANCA陽性のWGや，c-ANCA陽性となるMPA，CSSの報告もあり，好酸球やIgE定量，病理組織診なども併せて臨床的鑑別がなされる。病態に迫る抗体とし

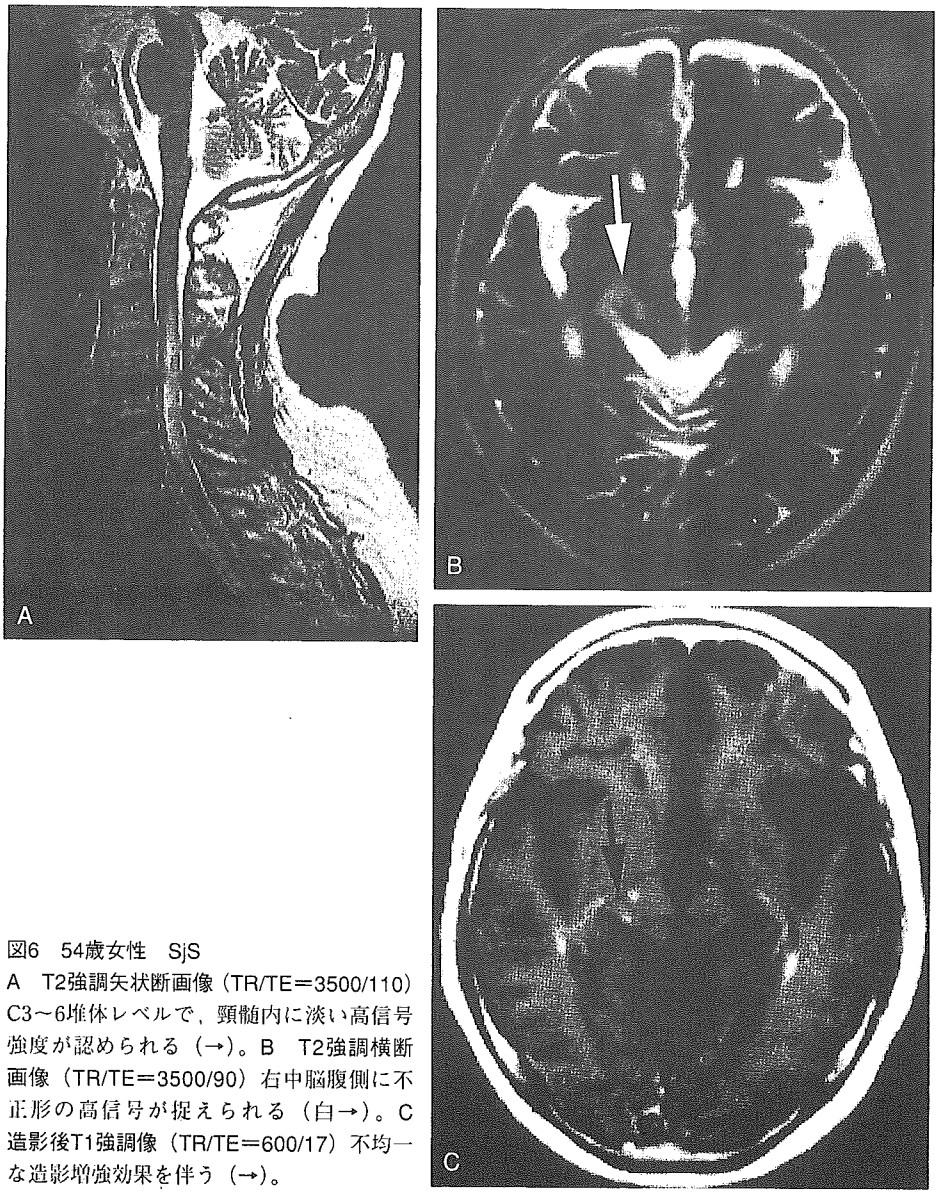

図6　54歳女性　SjS
A　T2強調矢状断画像（TR/TE＝3500/110）C3～6堆体レベルで，頸髄内に淡い高信号強度が認められる（→）。B　T2強調横断画像（TR/TE＝3500/90）右中脳腹側に不正形の高信号が捉えられる（白→）。C　造影後T1強調像（TR/TE＝600/17）不均一な造影増強効果を伴う（→）。

て，また，血管炎の分類を見直す契機となっているものとしての認識が現時点では大切と考えられる。

画像所見

中枢神経系の脳血管障害合併の報告は現在までのところ頻度の高いものではないが，血管炎を基礎とする小出血多発の病理報告等が認められ[9]，予後を規定する重要な因子として認識する必要がある。WG，CSSでも脳出血合併などの報告はあるが，むしろ髄膜の肥厚や実質内の肉芽腫形成などの報告が多く，それらの所見の合併をとらえることは，鑑別の重要なヒントとなる[10-12]。古典的多発動脈炎では脳血管炎の頻度は8%程度とされるが，脳出血，梗塞の報告が認められる。ANCA陽性の顕微鏡的多発血管炎での中枢神経障害の報告は少ないが，多発出血性梗塞をきたした報告がある[9]。ANCAという比較的簡便な検査法で検出できる指標が得られたことで，今後

さらに症例が積み重ねられるであろうし，通常の危険因子のな若年者の脳出血，梗塞などに対して，本症を一考する意義はあるだろう。

図7は，53歳女性。42歳時，左視床出血で発症。経過観察中のMR画像である。左視床にT2強調像で低信号を示す古い出血巣（図7→）が認められ，同様の病巣は右被殻にも捉えられる（図7→）。また両側放線冠，左被殻には，T2強調像で高信号を示す小病巣が散見されている。43歳時に発症した脳出血後，TIA様症状を繰り返し，不明熱，関節痛を伴い，抗核抗体4500倍以上，p-ANCA陽性，発症時より腎障害が認められ腎生検も施行された。臨床診断は顕微鏡的結節性多発動脈炎（microscopic polyarteritis nodosa，MPA）であった。

図8は，54歳女性。p-ANCA陽性のChurg-Strauss症候群例である。不明熱と激しい頭痛，視力障害を主訴とする。初回MRI，T2強調像では延髄左外側に高信号が認められる（図8A→）。造影後において，第4脳室外側溝，第4脳室背側に結節状の複数の造影増強効果を示す病巣が認められ（図8B），テント上では髄膜にも厚い造影増強効果が確認された。ステロイドと免疫抑制剤投与が施行され，1年後のMRでは，上記所見は軽快を示している（図8C）。髄膜，脈絡叢に肉芽形成，また延髄背側は梗塞というよりも肉芽形成に伴う浮腫などを見ていた可能性が考慮される。

図9は，52歳女性。c-ANCA一過性陽性，p-ANCA陽性のWG例である。両側中耳には炎症が存在し，右優位に厚い髄膜造影増強効果が認められる（図9A，B）。これらの画像所見は，ANCA測定のきっかけとなる事もあり，多彩な病像についての理解は大切である。

3. 橋本脳症（Hashimoto encephalitis）

橋本脳症は，橋本病を疑わせる高値の抗甲状腺抗体を有し，甲状腺機能は正常あるいは低下，臨床的に甲状腺機能低下のみでは説明しがたい急性，亜急性発症の意識障害，巣症状，痙攣などを呈する疾患群として報告が認められる。再発がありうる。甲状腺機能に依存せず，発症機序に自己免疫が絡んでいることが想定されている。剖検脳で肉眼的異常を指摘されなかった報告からは脳浮腫，また剖検例で脳幹の静脈にT-リンパ球浸潤が認められた報告からは免疫複合体沈着に基づく自己免疫性血管炎機序などが考えられている[13) 14)]。まれな疾患ではあるが，本症もステロイドの著効が知られており，迅速な診断の意義は大きい。Graves病での脳症の報告もあり，橋本脳症よりも「自己免疫性甲状腺疾患合併脳症：encephalopathy associated with autoimmune thyroid disease」と呼称する方が望ましいとする意見もある[15)]。

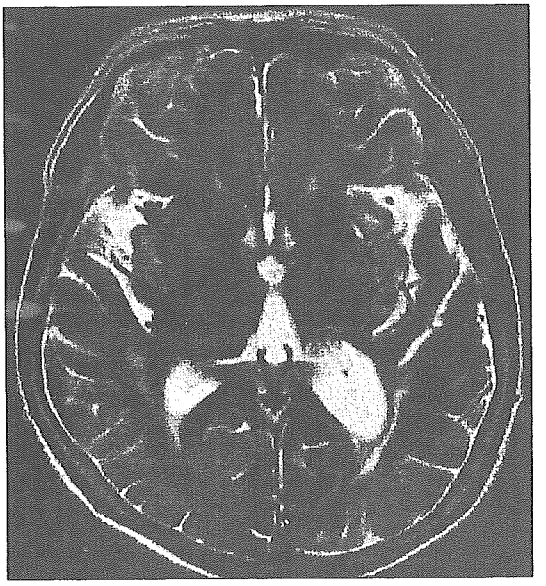

図7　53歳女性　MPA　T2強調横断画像（TR/TE＝4000/120）
左視床，右被殻などに複数の低信号強度が認められ，出血巣が疑われる。

画像所見

可逆性のびまん性皮質下白質信号異常，海馬領域，小脳白質，延髄などの腫脹を伴うFLAIR，T2強調像での高信号などの報告がある[16) 17)]病巣の局在は白質，皮質の双方に認められ，局在に特異的傾向は今のところ認められない。脳血流シンチでの血流低下が一過性に認められたとの報告もある。他の脳炎，虚血巣，腫脹のある急性期には腫瘍や肉芽腫との鑑別も考慮すること

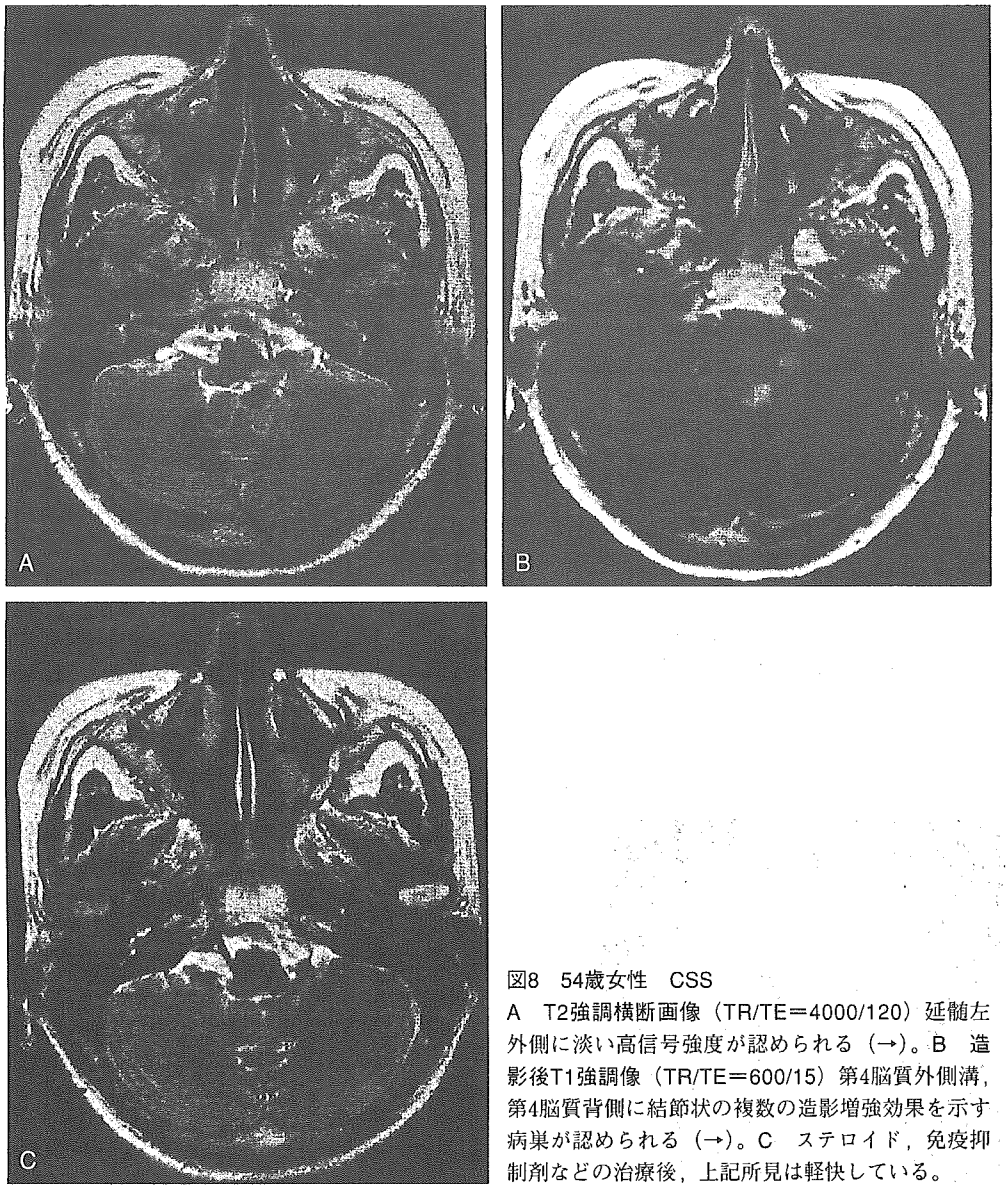

図8　54歳女性　CSS
A　T2強調横断画像（TR/TE＝4000/120）延髄左外側に淡い高信号強度が認められる（→）。B　造影後T1強調像（TR/TE＝600/15）第4脳質外側溝，第4脳質背側に結節状の複数の造影増強効果を示す病巣が認められる（→）。C　ステロイド，免疫抑制剤などの治療後，上記所見は軽快している。

になるが，小児を含めた若年者に原因不明の意識障害，痙攣などを認めた場合に，留意すべき疾患となる。Graves病に合併した脳症でMRAでの血管狭窄所見が，血漿交換療法後改善した報告[15]があり，免疫複合体沈着による血管炎が機序にあるとすれば橋本脳症でもMRAを検索する意義がありうるだろう。

図10は，23歳女性。痙攣，意識混濁の症例である。甲状腺機能は正常範囲にあったが，抗甲状腺抗体高値を示した。前頭葉皮質に多巣性に腫脹を伴うT2強調像での高信号が捉えられる。

4. リンパ球性下垂体炎（lymphocytic hypophysitis）

リンパ球性下垂体炎は，原因不明の下垂体の炎症性疾患である。妊婦や産褥期女性に合併することで知られていたが，年齢や性別，妊娠の有無との関係はむしろ希薄である。自己免疫性

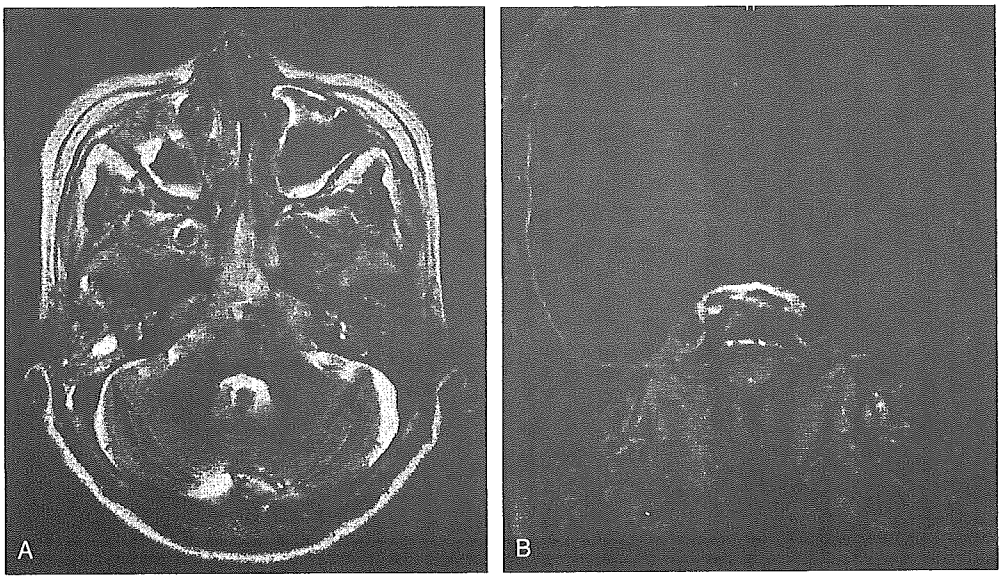

図9　52歳女性　WG
A　T2強調横断画像（TR/TE＝4000/120）両側中耳に不均一な高信号が認められ，中耳炎が疑われる（→）。B　造影後T1強調像（TR/TE＝600/15）右側優位に髄膜造影増強効果が広範囲に認められる（→）。

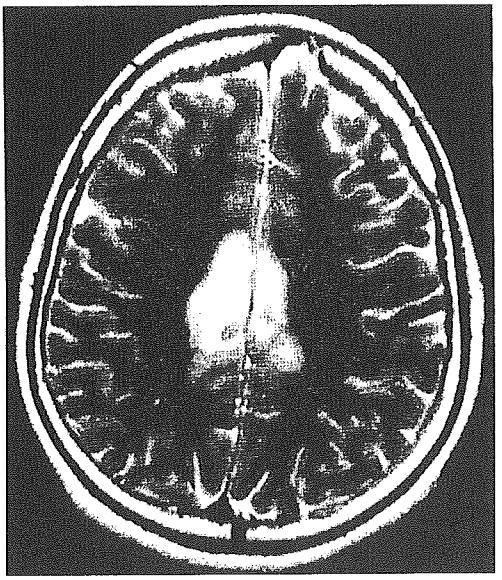

図10　23歳女性　痙攣，意識混濁　橋本脳症　T2強調横断画像（TR/TE＝3500/120）
前頭葉皮質に腫脹を伴う高信号強度が多巣性に認められる（→）。
（立川病院放射線科　白神伸之先生提供）

膵炎，慢性関節リウマチ，シェーグレン症候群，橋本病など自己免疫疾患の患者に発生率が高いとされ，自己免疫疾患を有する下垂体機能障害の診断において注意が必要と考えられる。

画像所見

下垂体前葉を主におかすもの（adenohypophysitis），下垂体柄や後葉などの神経下垂体に病変があるもの（infundibuloneurohypophysitis），腺神経下垂体ともに侵すもの（hypophysitis）などがあり，それぞれの部位の腫大，造影増強効果が認められる。周囲の髄膜造影増強効果合併は，炎症をより強く示唆する所見となる。サルコイドーシス，悪性リンパ腫などとの鑑別を要する場合がある。ステロイド治療が奏効する。図11は，34歳女性，生検によって（→は生検跡）リンパ球性下垂体炎が確認されている。下垂体，下垂体柄の腫脹，造影増強効果が認められるが（▲），1年後の画像では下垂体柄を含め腫脹の消退が確認される。

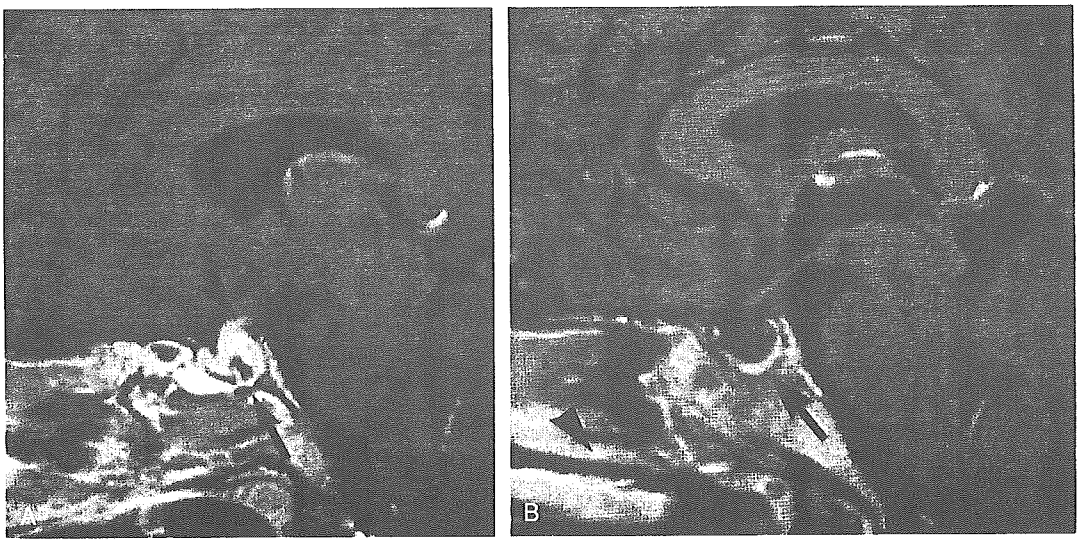

図11　34歳女性　リンパ急性下垂体炎
A　生検後の造影後T1強調矢状断画像（TR/TE＝600/15）→は生検痕を示す。下垂体前葉，下垂体柄の腫大，造影増強効果が（▲）認められる。B　1年後の画像　下垂体，下垂体柄の腫大は消失している。

おわりに

自己免疫疾患の中枢神経病変は，多彩かつ非特異的で，画像所見のみから“たった一つの病名あるいは病態”にたどり着くのは困難と思われるかも知れない。しかし，臨床診断に先行して意識障害で検査が施行されるような場合においてさえも，筆者達には，性別や年齢（推定でも），皮膚所見などの付帯情報は与えられている。何より，現在のMRIはその病巣の局在や性質について多くの情報を与えてくれる。ANCAやリンパ球性下垂体炎の項で触れたように，髄膜病変の付随を指摘するのは放射線診断医のみができうる役割だろう。まず所見を正確に拾い上げ，積み重ね，さらに正しく臨床情報を咀嚼し，放射線診断医としての意見をそのつど明確にしてゆくことが大切ではないかと考える。

（謝辞：橋本脳症画像を立川病院放射線科白神伸之先生にご提供いただきました。ここに深甚の謝意を表します。）

文　献

1）Nojima J et al：Strong correlation between the prevalence of cerebral infarction and the presence of anntiacardiolipin/β2-glycopppppprotein I and anti-phosphatidylserine/prothrombin antibodies. Thromb Haemost 91：867-876，2004
2）Nojima J：Association between anti-phospholipid antibodies and thrombotic complications in systemic lupus erythematosus. Rinsho Byori 51：239-247：2003
3）Jennings JE et al：Value of MRI of the brain in patients with systemic lupus erythematosus and neurologic disturbance. Neuroradiology 46：15-21，2003
4）Alexander EL et al：Magnetic Resonance Imaging of cerebral lesions in patients with the Sjögren syndrome. Annals of Internal Medicine 108：815-823，1988
5）Alexander EL et al：Primary Sjögren’s syndrome with central bervous system disease mimicking multiple sclerosis. Annal of Internal Medicine 104：323-330，1986
6）Ohtsuka T et al：Central nervous system disease in a child with primary Sjögren syndrome. J Pediatr 127：961-963，1995
7）Tajima Y et al：Neurological manifestations of primary Sjögren’s syndrome in Japanese patients. Internal Medicine 36：690-693，1997

8) Kadota Y et al：Primary Sjögren's syndrome initially manifested by optic neuritis；MRI findings. Neuroradiology 44；338-341，2002
9) 佐々木惇ほか：多発性出血性脳梗塞を呈したp-ANCA陽性顕微鏡的多発血管炎の1剖検例．脳神経 50：56-60，1998
10) Arbusow V，Samtleben W：Neurologic complications in ANCA-associated vasculitis. Dtsch Med Wochenschr 124：835-841，1999
11) Tokumaru AM et al：Intracranial meningeal involvement ini Churg-Strauss Syndrome. AJNR 23：221-224，2002
12) Murphy JM et al：Wegener Granulomatosis；MR imaging findings in brain and meninges. Radiology 213：794-799，1999
13) Nolte KW et al：Hashimoto encephalopathy；a brainstem vasculitis?. Neurology 54：769，2000
14) Oide T et al：Anti-neuronal autoantibody in Hashimoto's encephalopathy；neuropathological，immunohistochemical，and biochemical analysis of two patients. J of Neurol Sci 217：7-12，2004
15) Utku U et al：Reversible MR angiographic findings in a patient with autoimmune graves disease. AJNR 25：1541-1543，2004
16) Song YM et al：MR findings in Hashimoto encephalopathy. AJNR 25：807-808，2004
17) Bohnen NI et al：Reversible MRI findings in a patient with Hashimoto's encephalopathy. Neurology 49：246-247，1997

Summary

Central nervous system abnormalities in autoimmune disease；role of MRI

Autoimmune diseases are associated with several neurologic disorders such as encephalopathy，stroke like episodes and angitis etc. It is important to detect the lesions with MRI for evaluating the pathophysiology according to the clinical course，however，MRI findings of CNS abnormalities in autoimmune disease are sometimes non-specific. The purpose of this essay is to show various type of MRI abnormalities in autoimmune diseases.

Aya M Tokumaru et al
Department of Radiology
Tokyo Metropolitan Hospital of Gerontology

外国文献紹介

胆石に起因する膵炎の症例の管理においてMR胆管撮影が果たす役割について

Makary MA et al：The role of magnetic resonance cholangiography in the management of patients with gallstone pancreatitis. Ann Surg 241：119-124，2005

胆石に起因する膵炎は，しばしば総胆管結石を伴うため，腹腔鏡下胆嚢摘出術に先立って，内視鏡下の除去が必要になることがある。筆者らは，64例の胆石に起因する膵炎症例に対し，MR胆管撮影（MRC）を施行し，胆石，総胆管結石，胆嚢炎，膵炎について調べた。総胆管結石の有無はERCPによって確認した。その結果，17例が総胆管結石を伴っていたが，MRCで16例の結石を診断できた。また胆石は57例，急性膵炎は45例に認められた。そして，MRCは，胆石による膵炎の症例で，胆石の手術前に，総胆管結石の有無を正確に診断し，胆石や膵炎，胆嚢炎等の関連する疾患を調べる上で有用な手段と考えられると述べている。

瀬戸一彦

J Neuropathol Exp Neurol

Vol. 64, No. 12
December 2005
pp. 1118–1126

ORIGINAL ARTICLE

Unique Tauopathy in Fukuyama-Type Congenital Muscular Dystrophy

Yuko Saito, MD, PhD, Yasufumi Motoyoshi, MD, PhD, Takeshi Kashima, MD, PhD, Naotaka Izumiyama-Shimomura, PhD, Tatsushi Toda, MD, PhD, Imaharu Nakano, MD, PhD, Masato Hasegawa, PhD, and Shigeo Murayama, MD, PhD

Abstract

Fukuyama-type congenital muscular dystrophy (FCMD) is characterized by muscular dystrophy and cortical dysgenesis of the cerebrum and cerebellum. We investigated the extent and nature of tauopathy in the brains of 7 postfetal (14–34 years of age) and 2 fetal (18- and 20-week gestational age) FCMD cases. In all postfetal cases, tauopathy was found in the areas of cortical dysgenesis in the cerebrum, in addition to predictable sites such as the hippocampus. In fetal cases, the neuropil of malformed cerebral cortex was diffusely immunostained with anti-aberrantly phosphorylated tau antibodies. By immunoelectron microscopy, the epitope of the antibodies was associated with microtubule-like bundles within cellular processes protruding through disrupted glia limitans. In Western blot analysis, a unique 50-kDa band of tau was detected in a fetal and a postfetal case. In addition, 3 to 4 tau bands of 60 to 68 kD, similar to tau in Alzheimer disease, were also detected in the latter. After dephosphorylation, the insoluble tau from the fetal and the postfetal cases showed highly similar immunoblotting patterns. This anomalous phosphorylation of tau may be related to the development of the cortical dysgenesis in FCMD and may shed light on the biologic function of tau in the development of the central nervous system.

From the Department of Neuropathology (YS, SM), Tokyo Metropolitan Institute of Gerontology, Tokyo, Japan; the Department of Pathology (YS), Tokyo Metropolitan Geriatric Hospital, Tokyo, Japan; the Department of Neurology (YM), National Shimoshizu Hospital, Chiba, Japan; the Department of Human Pathology (TK), Graduate School of Medicine, University of Tokyo, Tokyo, Japan; the Human Tissue Research Group (NI-S), Tokyo Metropolitan Institute of Gerontology, Tokyo, Japan; the Division of Clinical Genetics (TT), Department of Medical Genetics, Osaka University Graduate School of Medicine, Osaka, Japan; the Department of Neurology (IN), Jichi Medical School, Tochigi, Japan; and the Department of Molecular Neurobiology (MH), Tokyo Institute of Psychiatry, Tokyo, Japan.

Send correspondence and reprint requests to: Shigeo Murayama, MD, PhD, Department of Neuropathology, Tokyo Metropolitan Institute of Gerontology, 35-2 Sakaecho, Itabashi-ku, Tokyo 173-0015, Japan; E-mail: smurayam@tmig.or.jp

Supported by Aid for Scientific Research on Priority Areas—Advanced Brain Science Project—from the Ministry of Education, Culture, Sports, Science and Technology of Japan (SM, YS); Aid for Degenerative Disease from Ministry of Health, Labor, and Welfare (SM); and Aid for a Long-Term Comprehensive Research on Age-Associated Dementia from Tokyo Metropolitan Institute of Gerontology (SM).

Key Words: Fukutin, Glia limitans-basal lamina complex, Gliomesenchymal tissue, Malformation, Polymicrogyria.

INTRODUCTION

Fukuyama-type congenital muscular dystrophy (FCMD; MIM 2533800) is the second most common muscular dystrophy next to Duchenne muscular dystrophy in Japan. An autosomal-recessive disorder, FCMD is characterized by severe congenital muscular dystrophy associated with brain malformation, principally cerebral and cerebellar cortical dysgenesis (1, 2). Recently, the FCMD gene was identified on chromosome 9q31 and its gene product was named *fukutin* (3). However, the role of *fukutin* in various clinical presentations of FCMD remains to be clarified.

The neuropathology of FCMD is characterized by polymicrogyria of the cerebrum and cerebellum, pachygyria, agyria, and anomalies of the pyramidal tracts (2) and is categorized as type II lissencephaly (4). A migration disorder during the period of brain development is thought to cause these brain abnormalities (2, 5). Microscopically, the surface of the brain in FCMD cases is covered with neurogliomesenchymal tissue (nGMT) containing mixtures of neuronal and glial tissue. We and others have recently reported that there are breaches of the glia limitans–basal lamina complex of the brains and in the skeletal muscles in fetal (6, 7) and postfetal (8, 9) cases.

Neurofibrillary tangles (NFTs) have been reported in FCMD cases in the locus ceruleus, basal nucleus of Meynert (10), and hippocampus (11), and thus FCMD has been classified as a secondary tauopathy along with muscle diseases such as myotonic dystrophy, hamartomatous diseases such as tuberous sclerosis (12), and infections such as subacute sclerosing panencephalitis (13), as well as metabolic diseases such as Niemann-Pick type C disease (14) and Salla disease (15). However, the phosphorylation of tau in these cases has not been fully studied except in a few examples such as Niemann-Pick type C disease (16) and myotonic dystrophy (17).

Here we examined both fetal and postfetal cases of FCMD neuropathologically and biochemically and found accumulation of aberrantly phosphorylated tau in the malformed tissue from both groups. The immunochemical analysis of the insoluble tau from the fetuses and postfetal cases revealed that it included a unique band that was distinct from the insoluble tau from typical Alzheimer disease (AD). Our

study may shed new light on the roles of tau as well as *fukutin* in the developing human brain.

MATERIALS AND METHODS

Nine cases of FCMD were examined in this study, including 2 fetal cases (18 and 20 weeks gestational age) and 7 postfetal cases (14–34 years of age, with mean 22.9 ± 6.4 years of age, 6 males and one female). The profiles of the FCMD cases are summarized in Table 1. All postfetal cases had muscular dystrophy as well as brain malformation accompanied by a defect in the basal lamina, fulfilling the morphologic diagnostic criteria for FCMD (6, 9). Cases 1, 3, 4, 6, 7, and 8 were also used in our previous studies (6, 8). Two control fetal cases (23 and 24 weeks gestational age), 5 neurologically unremarkable age-matched postfetal cases (28–43 years of age, 3 females and 2 males), 5 AD cases (based on NIA-Ronald Reagan Institute Criteria) (18), and an 89-year-old man with incidental polymicrogyria served as controls. The 2 FCMD fetuses were aborted at their parents' request as a result of a prenatal diagnosis of FCMD based on the results of microsatellite polymorphism analysis of the fetal DNA (19, 20). The 2 control fetal cases were therapeutically aborted because of the maternal medical condition. Informed written consent for the use of the autopsy materials for research was obtained for all the cases examined.

Neuropathology

The brain, spinal cord, and pieces of skeletal muscle were sampled for examination. Half of the brain of case no. 1 and the frontal lobe of cases 2, 6, and 9 were kept frozen for biochemical and molecular studies. Pieces of the frontal lobe and the cerebellum from cases 2, 5, 6, and 9 were fixed in 2.5% glutaraldehyde for ultrastructural studies. Pieces of the frontal and occipital lobes and hippocampus from case no. 9 were fixed in 4% paraformaldehyde for 48 hours and embedded in paraffin. The rest of the brain and spinal cord were fixed in 10% buffered formalin and sliced in the coronal plane at approximately 8- to 10-mm thickness. After macroscopic observation, the appropriate areas were embedded in paraffin.

Six-μm-thick sections were stained with hematoxylin and eosin (H&E), Klüver-Barrera, and Bodian silver staining, periodic acid-methenamine (PAM), Watanabe, Bielschowsky, and Gallyas-Braak (21) methods.

Immunohistochemistry

After deparaffinization, 6-μm-thick sections were processed for single or double immunostaining using an automatic immunostainer (Ventana 20NX, Tucson, AZ) (22, 23). The following anti-tau antibodies were used for the study: AT8, phosphorylated Ser-202/Thr-205 (Innogenetics, Temse, Belgium); AP422, phosphorylated Ser-422 (a gift from Dr. Y. Ihara); and PHF1, Ser-396/404 (a gift from Dr. P. Davies). Also used were antiubiquitin (Sigma, St. Louis, MO), anti-Aβ (12B2, a.a. 11-28; IBL, Maebashi, Japan), antiphosphorylated α-synuclein (psyn#64, a gift from Dr. T. Iwatsubo), antiphosphorylated neurofilament (SMI 31; Sternberger Monoclonals Inc., Baltimore, MD), antimicrotubule-associated protein 2 (HM-2, Sigma), anticollagen type IV (CIV22; DAKO, Carpinteria, CA), antiglial fibrillary acidic protein (GFAP; Sigma), and antiHLADR (CD68; Sigma) antibodies. The specimens were prepared without the primary antibodies as negative controls.

Ultrastructural Study

Small pieces of the frontal lobe and cerebellar cortex from cases 1, 5, and 9 and the hippocampus from case 9 were fixed in 2% glutaraldehyde, postfixed in 1% osmium tetroxide, and embedded in epoxy resin. One-micrometer-thick semithin sections were stained with toluidine blue and an appropriate area was trimmed for ultrastructural observation.

Immunoelectron Microscopic Study

Ten percent buffered formalin-fixed, paraffin-embedded frontal lobe samples from the 2 fetal FCMD cases as well as the 2 controls were cut at 30-μm thickness, placed on Aclar film (Nisshin EM, Tokyo, Japan), and immunostained with

TABLE 1. Case Profiles of Fukuyama-Type Congenital Muscular Dystrophy

Case No.	Age	Gender	PMI (hours)	BW (g)	Gait	Epilepsy	Mutation in Fukutin Gene
1	18 gw	N/A	N/A	20†			Arg 47 Stop (exon3), insertion
2	20 gw	M	4.2	40†			Insertion: homozygous
3	14 years	M	12	N/A	Impossible	−*	N/E
4	19 years	M	N/A	N/A	Ambulant until age 2 years	−	N/E
5	21 years	M	2	1,400	Impossible	+	Insertion: homozygous
6	21 years	M	2	1,350	Ambulant until age 9 years	−	Insertion: homozygous
7	24 years	M	5.5	1,160	Ambulant until age 7 years	+	N/E
8	27 years	F	N/A	N/A	Impossible	−*	N/E
9	34 years	M	5	1,350	Impossible	−	Insertion: homozygous

gw, gestational week; PMI (h), postmortem interval (hours); BW, brain weight; N/A, not available; Insertion, retrotransposal insertion; −*, electroencephalography showed abnormal discharge without epilepsy; N/E, not examined. †, The brain weight of normal controls (mean ± standard deviation) estimated by gestational weeks was 29.4 ± 8.4 g for 18 weeks and 45.5 ± 11.3 for 20 weeks ([31]).

antiphosphorylated tau protein (AT8 and AP422) using the avidin-biotin-peroxidase complex method (8). After the samples were fixed with 2% glutaraldehyde, postfixed in 1% osmium tetroxide, and embedded in epoxy resin, appropriate areas were trimmed and observed with an electron microscope (JEOL 2000EX, Tokyo, Japan). The specimens were prepared without the primary antibodies as negative controls.

Immunoblot Analysis of Phosphorylated tau

Sarkosyl-insoluble tau was extracted from fresh-frozen brains of patients with FCMD (cases 1 and 9), AD, and from a one-day-old rat. The tissues were homogenized with a polytron homogenizer in 10 volume (w/v) of buffer consisting of 10 mM Tris-HCl (pH 7.4), 0.8 M NaCl, 1 mM EGTA, and 10% sucrose and centrifuged for 15 minutes at 3,000 rpm (1,000 × g). The supernatants were retained and ultracentrifuged for 20 minutes at 800,000 rpm (390,000 × g). The pellets were resuspended in 10 volume (w/v) of homogenization buffer by sonication, brought to 1% Sarkosyl (w/v), and incubated for 1 hour at room temperature. After a 20-minute ultracentrifugation, the pellets were resuspended in 0.2 mL of 50 mM Tris-HCl (pH 7.4) per gram of starting material and used for immunoblotting. Aliquots were electrophoresed on 10% SDS-polyacrylamide gels, transferred to Immobilon membranes, and immunoblotted with anti-tau antibody, tau C (430-441), and HT7 (Innogenetics), and visualized by the avidin-biotin-peroxidase complex method (24, 25).

RESULTS

Macroscopic

Fetuses

The brain weight of the 2 fetal cases of FCMD was 20 g and 40 g, respectively. The surface of the brain showed extensive fine wrinkles over the cerebral cortex with frequent small verrucous regions (Fig. 1A, B) as has been previously reported (6).

Postfetal Cases

The brain weights of cases 5, 6, 7, and 9 were 1,400 g, 1,350 g, 1,160 g, and 1,350 g, respectively (Table 1). The brain weights of cases 3, 4, and 8 were not available. Bilateral cerebral and cerebellar polymicrogyria, accentuated in the frontal lobe and the cerebellar hemisphere, was seen to various degrees (Fig. 1C). Pachygyria involving the parietal and occipital lobes was also observed in cases 8 and 9 (not illustrated). In the serial coronal sections, fusion of the adjoining gyri was often present in the frontal lobe, where polymicrogyria was seen in all cases. In one of the control cases, incidental polymicrogyria with a similar structure was found in the parietal lobe.

Light Microscopy Study of Cortical Dysgenesis

Fetuses

The histologic features of both fetal cases of FCMD (Fig. 2) were essentially similar and therefore are described together. The cerebral cortex was diffusely covered by neurogliomesenchymal tissue (nGMT) (Fig. 2A, B) (6). The nGMT was thicker in case 2 than in case 1. The neuroglial elements located in the nGMT appeared to have migrated outward through multiple breaches of the glia limitans (Fig. 2B). The majority of the small blood vessels entered into the cortical plate from the nGMT through the breaches, although some of them appeared to penetrate into the cortical plate through intact segments of the glia limitans. In addition to heterotopic cortical plate neurons, the nGMT contained a few

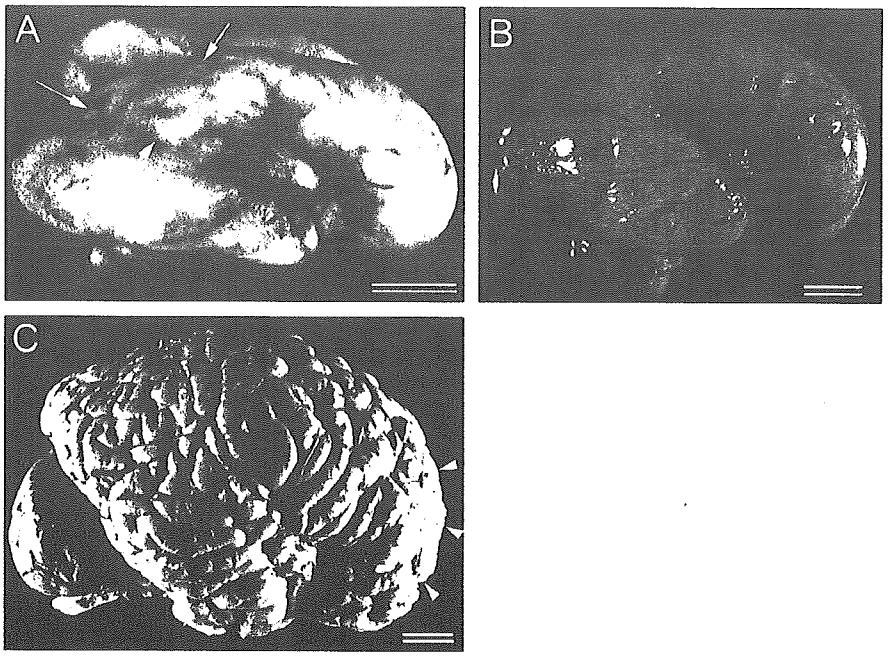

FIGURE 1. Macroscopic findings of the Fukuyama-type congenital muscular dystrophy brain. **(A)** A fetal case of Fukuyama-type congenital muscular dystrophy with extensive fine wrinkles over the cerebral cortex with frequent small verrucous regions (arrows) (case 2) Scale bar = 5 mm. **(B)** A normal control fetus (23-week gestational age). **(C)** A postfetal case (case 6) with typical polymicrogyria (arrowheads). Scale bar = 2 cm.

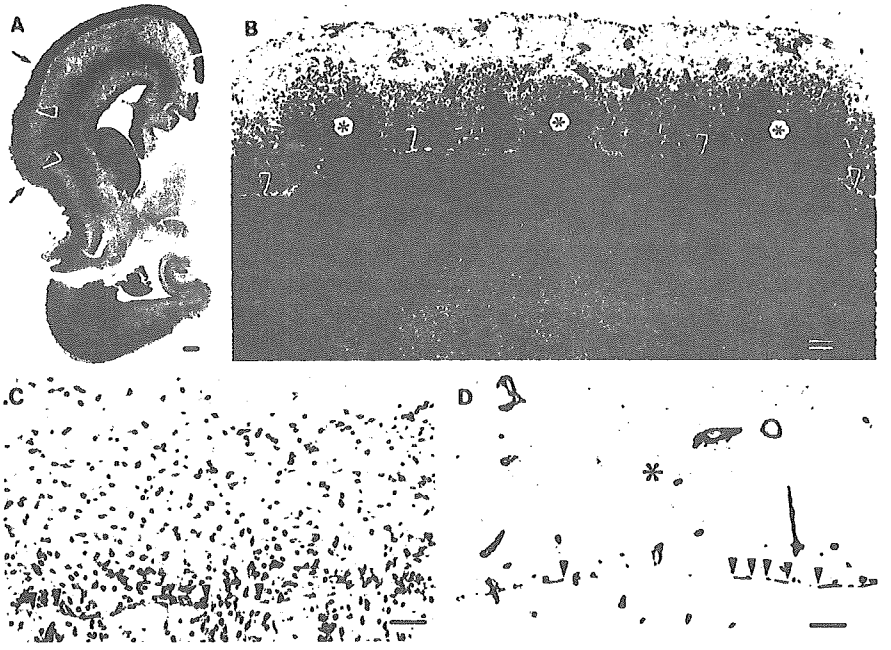

FIGURE 2. Microscopic findings of brain malformation in a fetal Fukuyama-type congenital muscular dystrophy case (case 2). **(A)** A coronal section of the left hemisphere at the hippocampus (hematoxylin & eosin). Gliomesenchymal tissue (arrows) with outer placement of the granular layer (arrowheads). Scale bar = 1 mm. **(B)** Higher magnification of the area indicated by arrowheads in the panel (A). Asterisks indicate brain tissue protruding into the neurogliomesenchymal tissue (nGMT). Arrowheads indicate glia limitans (GL) and basal lamina (BL) complex. Scale bar = 100 μm. **(C)** Disruption of the GL-BL complex (arrowheads) visualized by GFAP immunostaining in the interface to the nGMT. Scale bar = 100 μm. **(D)** The disruption of the GL-BL complex detected immunohistochemically with anticollagen type IV antibody. Asterisk indicates nGMT and arrowheads show GL-BL complex. Scale bar = 100 μm.

deeply located Cajal-Retzius cells, subpial granular layer cells, and glial cells. In the parts of the cerebral cortex where the glia limitans was well preserved, the cortical architecture was normal. The breaches of the glia limitans were frequently detected in the frontal, temporal, and parietal lobes but were rare in the occipital cortex. In the cerebellum, the continuity of the outer granular cell layer was disrupted and clusters of granular cells were present in the subpial layer, where the cortex was covered by nGMT. In the cerebellar hemisphere, the structure partially resembled cerebellar polymicrogyria in the postfetal cases. The glia limitans in the cerebral cortex was immunoreactive to anticollagen type IV and GFAP antibodies, and had frequent breaches in the frontal, temporal, and parietal lobes (Fig. 2C, D).

Postfetal Cases

In the area with macroscopic polymicrogyria, nGMT (including neural and glial tissue) covered the brain surface. The adjoining gyri were fused by obliteration of the subarachnoid space with nGMT and the meningeal vessels were entrapped. Within this nGMT, haphazardly scattered ectopic neurons were detected, especially in the temporal lobe. In the immunohistochemical study, breaches of the glia limitans in the cerebral cortex were seen with anti-GFAP and collagen type IV antibodies. nGMT itself was also immunoreactive to anti-GFAP antibody.

Light Microscopy Study of Tauopathy

Fetuses

Gallyas-Braak silver staining was weakly positive in the neural tissue protruding from the breaches of the glia limitans, but no reaction was obtained with the Bodian or Bielschowsky method. In case 2, the argyrophilic structures appeared to be aggregated in the superficial layer of the nGMT. Immunohistochemically, AT8 and PHF1, which recognize the fetal phosphorylation site of tau, reacted with the parenchyma of both FCMD and control cases. However, AP422, which recognizes an abnormal phosphorylation site of tau that is present in AD but absent from fetuses (24), reacted only with the brains from FCMD cases (Fig. 3). The immunoreactivity was not observed in the negative controls processed without the primary antibodies (data not shown). The AP422-positive structures protruded from the breaches of the glia limitans and appeared to aggregate in the superficial layer of the nGMT in case 2. The AP422-immunoreactive structures in the nGMT were also stained with SMI 31 but not with anti-GFAP antibody, indicating that these structures were of neuronal, not glial, origin.

Postfetal Cases

NFTs and neuropil threads, visualized by silver staining, were present in the hippocampus, entorhinal and transentorhinal cortex, locus ceruleus, and basal nucleus of Meynert in all of the postfetal cases examined. The number and extent of NFTs were commensurate with age in cases 5, 6, 7, and 9. When the Braak staging for NFTs was applied, the younger cases (cases 5 and 6) were classified into the entorhinal stage, and the oldest case (case 9) was classified into the limbic stage (26). In addition, a small number of NFTs were scattered in the frontal and temporal lobes, cingulate gyrus, insular cortex, raphe nucleus, dentate nucleus, substantia nigra, and spinal anterior horn cells. Moreover, NFTs were also present in the ectopic neurons (Fig. 4A) within the abnormal nGMT. Swollen dendrites packed with NFTs were frequently seen (Fig. 4B).

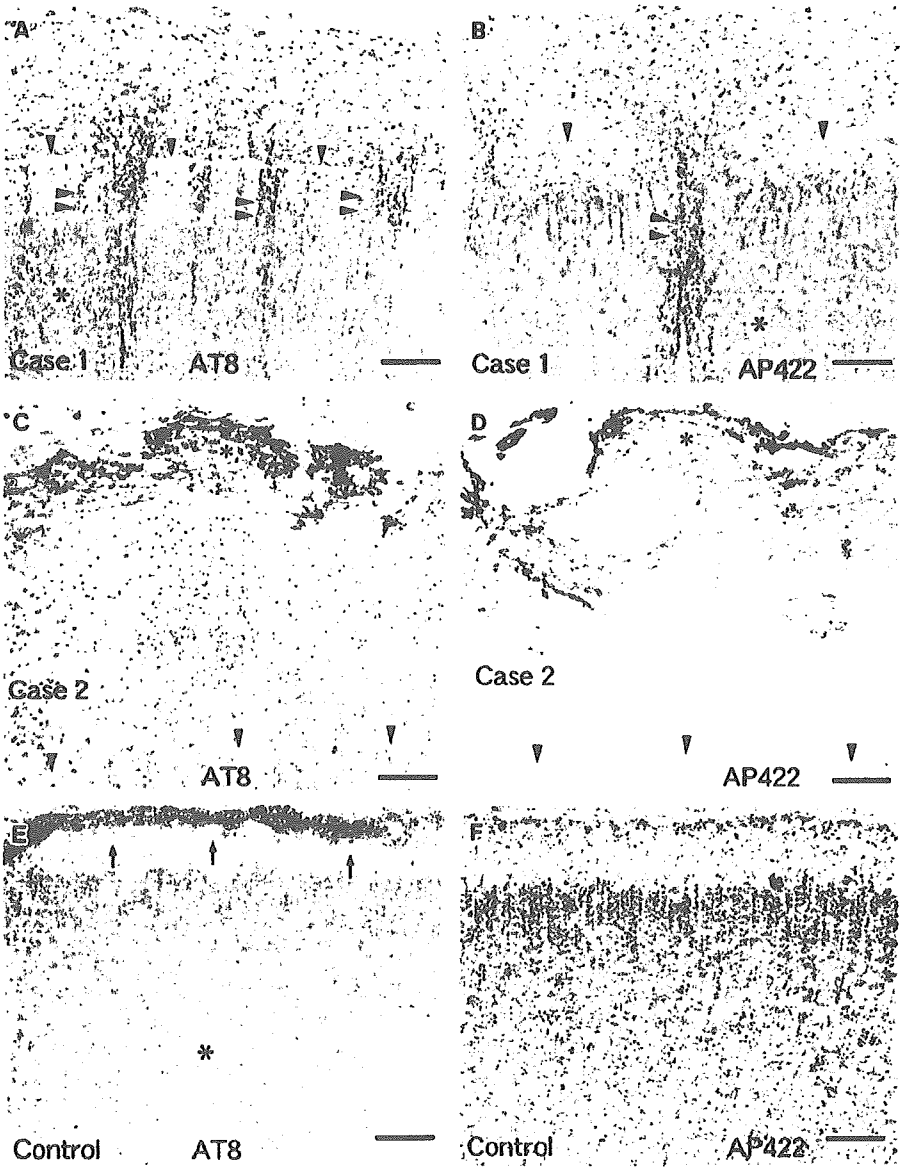

FIGURE 3. Tauopathy in the Fukuyama-type congenital muscular dystrophy fetal brains. **(A)** The AT8-immunoreactive protruding tissue (double arrowheads) from the parenchyma (asterisk) through breaches in the glia limitans (GL) and basal lamina (BL) complex (arrowheads, case 1). **(B)** The same pattern in immunostaining with AP422. Arrowheads indicate GL-BL complex and double arrowheads, protruding neural tissues from the brain parenchyma (asterisk). **(C)** AT8-immunoreactive ectopic tissue (asterisk). Arrowheads indicate GL-BL complex (case 2). **(D)** The same pattern in immunostaining with AP422. The asterisk indicates AP422-positive nGMT and arrowheads indicate GL-BL complex. **(E)** Superficial AT8 immunoreactivity in a control fetus. Arrows indicate the surface of the brain and asterisk, the deep cortical layer. **(F)** No immunoreactivity with AP422 in the control fetal brain (the same area in panel **[E]**). Scale bar = **(A–F)** 100 μm.

Immunohistochemical studies with antiphosphorylated tau antibodies detected more widespread abnormal structures than the silver staining methods in the malformed tissue as well as structures with apparently normal development in all the postfetal cases (Fig. 4C–G). The former included the area of the cortical fusion, nGMT, the ectopic neuronal tissue in the cerebral subpial layer, and the perivascular area (Table 2), including those in the younger cases (cases 3 and 4), but did not include the cerebellar polymicrogyria.

Neither anti-Aβ nor antiphosphorylated α-synuclein antibodies stained any structure. In the case of incidental polymicrogyria (89-year-old man), phosphorylated tau-positive

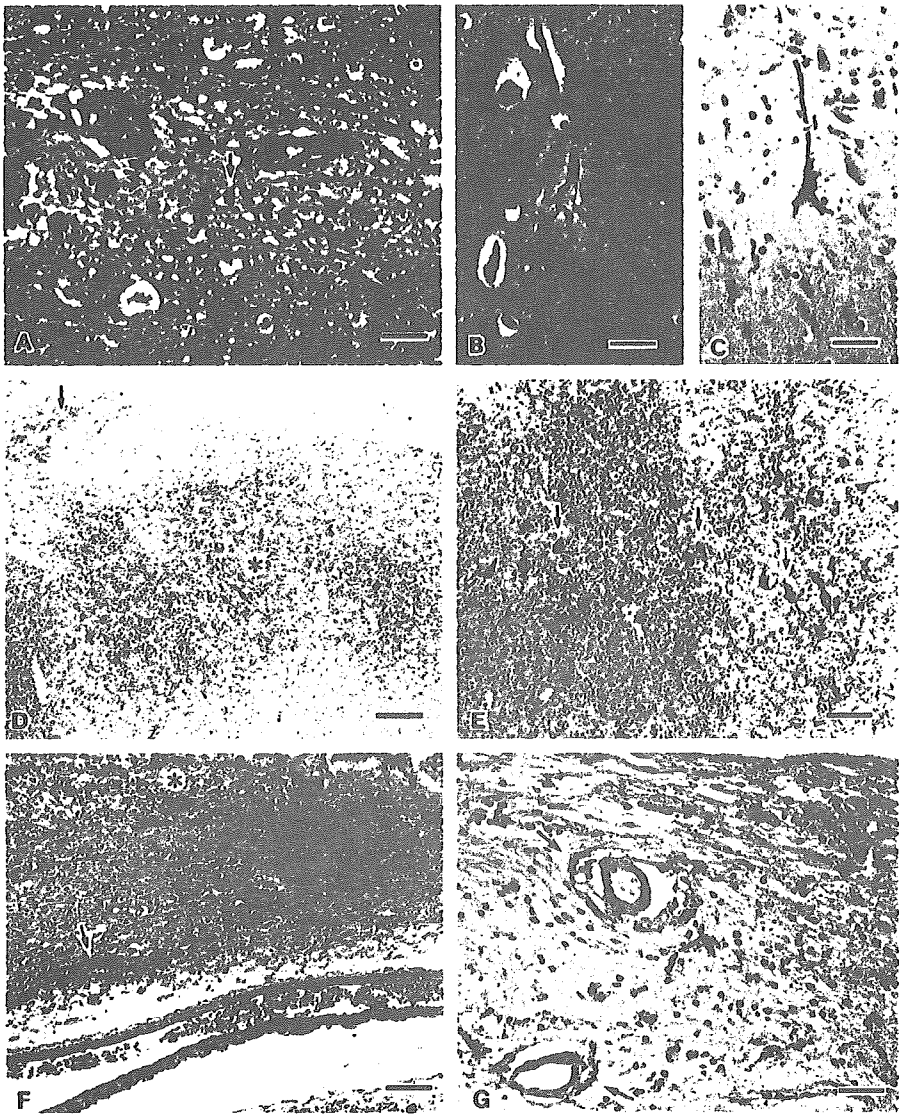

FIGURE 4. Tauopathy in postfetal cases of Fukuyama-type congenital muscular dystrophy. **(A)** Neurofibrillary tangles (NFT) (arrow) in the area of adhesion (case no. 8). Scale bar = 40 μm. **(B)** An NFT in an ectopic neuron in the hippocampus. Scale bar = 40 μm. **(C)** Serial section of panel **(B)**. AT8 immunostaining. Scale bar = 40 μm. **(D)** In addition to diffuse staining of the parahippocampal gyrus (asterisk), ectopic tissue including neuronal cytoplasm (arrow) shows AT8-immunopositive staining. Scale bar = 200 μm. **(E)** Neurofibrillary tangles (arrows) and neuropil threads visualized by AT8 immunostaining in the parahippocampal gyrus. Scale bar = 100 μm. **(F)** Ectopic tissue (asterisk) as well as perivascular area (arrow) showing positive AT8 immunostaining. Scale bar = 100 μm. **(G)** Ectopic tissue from the temporal lobe (AT8 immunostaining). The arrow indicates immunoreactive perivascular tissue. Scale bar = 100 μm.

structures were seen only in the entorhinal and transentorhinal areas, but not in the area of polymicrogyria.

Electron Microscopic Study

Fetuses

In the nerve processes protruding into the nGMT from the breaches of the glia limitans, bundles of microtubules were seen but no paired helical filaments (PHFs) were identified (Fig. 5A). An immunoelectron microscopic study demonstrated both AT8- and AP422-immunoreactive tubules in the same area (Fig. 5B). No immunostaining was detected either in the normal controls or the negative controls processed without the primary antibodies (data not shown).

Postfetal Cases

NFTs composed of PHFs were seen in the hippocampus from cases 7 and 8 (Fig. 6B). Anomalously shaped NFTs were only seen in FCMD cases. Hirano bodies (data not shown) and granulovacuolar changes were also seen in FCMD cases (Fig. 6A).

TABLE 2. Summary of Phosphorylated Tau-Related Structures in Relation to Cerebral Cortex

	Ptau-Immunoreactive Structures				Neurofibrillary Tangles			
Case No.	Limbic Regular	Limbic Ectopic	Neocortex Regular	Neocortex Ectopic	Limbic Regular	Limbic Ectopic	Neocortex Regular	Neocortex Ectopic
1	+	+	+	+	–	–	–	–
2	+	+	+	+	–	–	–	–
3	+	+	–	–	–	–	–	–
4	+	+	+/–	+/–	–	–	–	–
5	+	+	+	+	+	+	–	+
6	+	+	+	+	+	+	–	+
7	++	++	+	+	++	++	+	+
8	++	++	+	+	++	++	++	+
9	++	++	+	+	++	++	++	+

Ptau, phosphorylated tau.

Immunoblotting With Anti-tau Antibodies

A unique 50-kD band was present in a fetal FCMD case and was very weakly detected in a rat fetus used as a control (Fig. 7). In a postfetal case of FCMD (case 9), there were 3 major bands of tau: 60, 64, and 68 kD that were similar to pathologic tau in AD, plus some minor bands, as well as a 50-kD band similar to the 50-kD band observed in the fetal FCMD case. After dephosphorylation, the insoluble tau from

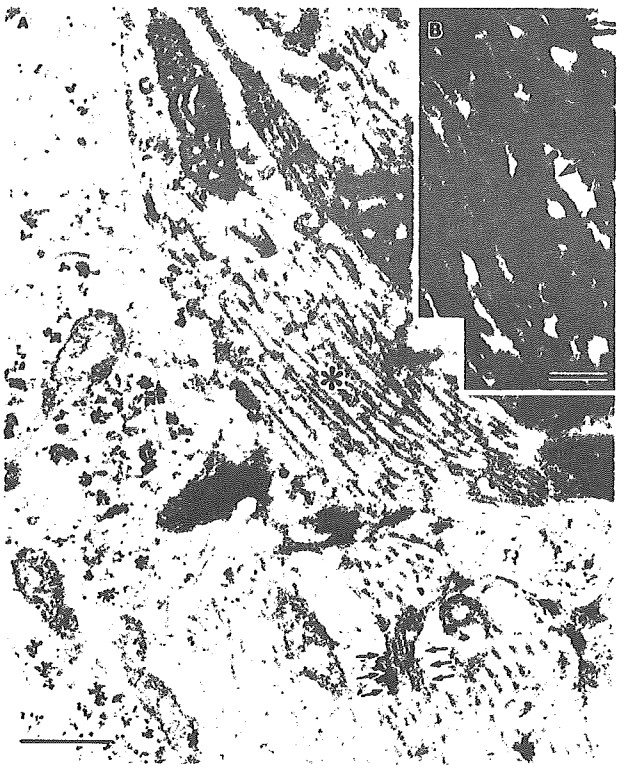

FIGURE 5. Ultrastructure of the antiphosphorylated tau-immunoreactive structure in a fetal case of Fukuyama-type congenital muscular dystrophy (case 1). **(A)** Higher magnification of the neural tissue protruding from glia limitans–basal lamina complex. Microtubules (asterisk) with focal constriction (arrows). Scale bar = 500 nm. **(B)** The tubules in the protruding tissue, decorated by AP422 (arrow) (avidin-biotin complex preembedding method). Scale bar = 500 nm. The decoration was abolished by skipping the application of APP422.

FIGURE 6. Ultrastructure of neurofibrillary tangles (NFT) in a postfetal case of Fukuyama-type congenital muscular dystrophy (case 6). **(A)** NFT-bearing neuron. "G" indicates the granulovacuolar degeneration. Scale bar = 500 nm. **(B)** Higher magnification of NFTs indicated in panel **(A)**, which consists of paired helical filaments (arrowheads) identical to those observed in Alzheimer disease. Scale bar = 200 nm.

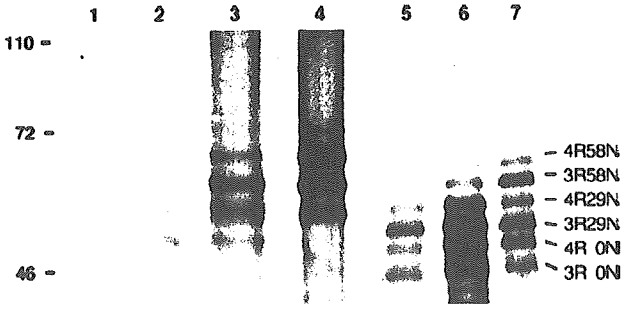

FIGURE 7. Biochemical analysis of tau in Fukuyama-type congenital muscular dystrophy (FCMD) brains. Immunoblots of sarkosyl-insoluble tau from one-day-old rat (lane 1), FCMD fetus (lane 2), FCMD postfetal case (lane 3), and Alzheimer disease (AD) (lane 4) brains with anti-tau antibody Tau C (430–441) and the sarkosyl-insoluble fraction after dephosphorylation stained with HT7. Note the presence of a 50-kD band in the fetal case of FCMD (lane 2), whereas there is only a very weak corresponding band in the fetal rat as a control (lane 1). In the postfetal case of FCMD (lane 3), 3 major tau bands of 60, 64, and 68 kD, which are similar to pathologic tau in AD (lane 4), plus some minor bands, as well as the 50-kDa band similar to that in the fetal FCMD case, were detected in the sarkosyl-insoluble fraction. After dephosphorylation, tau from the fetal (lane 5) and postfetal (lane 6) FCMD cases showed similar immunoblotting patterns and were richer in 3-repeat tau than was tau from AD (lane 7).

the fetus and the postfetal cases showed highly similar immunoblotting patterns and were more enriched in three-repeat tau than the insoluble tau from typical AD cases.

DISCUSSION

We report here for the first time a widespread tauopathy, or aberrant phosphorylation of tau, associated with brain malformation in fetal as well as postfetal cases of FCMD. The aberrant phosphorylation of tau in the malformed brain may be related to the abnormality of axonal development. It is not clear whether the 50-kDa band is of primary or secondary significance; however, it is common to both fetal and postfetal cases of FCMD. It is reasonable to assume that the 50-kD band observed in Western blots may correspond to the diffuse immunostaining in the neuropil of the malformed tissue with antiphosphorylated tau antibodies in both the fetal and the postfetal cases. Although only one fetal and one postfetal case were analyzed and no data were obtained for the brains of the control fetuses, the 50-kDa bands found in both in the fetal and postfetal FCMD are probably worthwhile reporting at this time in view of the difficulty of obtaining further tissues for analysis.

The location of aberrantly phosphorylated tau on structures similar to microtubules in the fetal case may indicate the loss of dynamic stability of microtubules in the abnormal environment. In FCMD cases, a tau band with an apparent molecular weight of 50 kDa was detected in the insoluble fraction. The lower molecular weight is likely to represent a lower level of tau phosphorylation because no degradation band was observed after dephosphorylation. These results suggest that the level of tau phosphorylation in the fetal stage, which is lower than the phosphorylation level in AD brains, may be sufficient to cause the accumulation of tau in FCMD brains. In FCMD, the aggregated (accumulated) tau may be converted to the filamentous form of the aggregates by further phosphorylation. It may also promote PHF formation by acting as a kind of seed.

The causative gene for FCMD has been shown to be expressed in developing neurons in the fetal brain by immunocytochemistry (27) and in situ hybridization (28), and is expressed at a lower level in the glia cells (29). More recently, congenital muscular dystrophies, which are said to be caused by defects in known or putative glycosyltransferases, have been shown to be commonly associated with hypoglycosylation of α-dystroglycan and a marked reduction of its receptor function (30). At present, fukutin is thought to play a cofactor role in glycosyl transfer at the Golgi membrane (Xiong et al, unpublished data). Because neuron-specific ligands for α-dystroglycan have been identified (31), fukutin may play a crucial role in neuronal migration by interacting with glycosyl residues in the matrix. Because several reports have indicated a direct link between abnormal protein glycosylation and aberrant phosphorylation of tau (32), fukutin could also play a role in the integrity of microtubules, a major cytoskeletal structure in neurite growth. Thus, the altered metabolism of tau in the malformed tissue of FCMD may represent a downstream event of the mutation of *fukutin* in the developing brain.

The phosphorylated insoluble tau from AD was reported to be similar to that from Niemann-Pick type C disease (16) but different from that from myotonic dystrophy (17). The phosphorylated tau from FCMD was apparently richer in three-repeat tau and less phosphorylated than that from AD. Although the formation of NFTs is a final common pathway of cytoskeletal alterations common to AD, the process of reaching that point may involve abnormal processing of tau that is specific to each original pathologic process. Thus, the study of tau in FCMD could provide new evidence about the pathogenesis of NFT formation.

ACKNOWLEDGMENTS

The authors thank Dr. Yasuo Ihara (Department of Neuropathology, University of Tokyo, Tokyo, Japan), Dr. Peter Davies (Department of Pathology, Albert Einstein College of Medicine, Bronx, New York), and Dr. Takeshi Iwatsubo (Department of Neuropathology and Neuroscience, Graduate School of Pharmaceutical Science, University of Tokyo, Tokyo, Japan) for the donation of antibody; Mr. Hiroyuki Kashima, Ms. Junko Saishoji, Mr. Naoo Aikyo, Ms. Mieko Harada, and Ms. Nobuko Naoi for the preparation of sections; and Dr. Kinuko Suzuki (Department of Pathology and Laboratory Medicine, University of North Carolina at Chapel Hill, North Carolina) for helpful discussions and comments. Part of this study was presented at the 80th Annual Meeting of the American Association of Neuropathologists, Inc. held in Cleveland, Ohio, June 2004.